Journal of Gerontology: BIOLOGICAL SCIENCES
2006, Vol. 61A, No. 3, 218–231

BMP REF 9

Gene Expression and Physiologic Responses of the Heart to the Initiation and Withdrawal of Caloric Restriction

Joseph M. Dhahbi, Tomoshi Tsuchiya, Hyon-Jeen Kim, Patricia L. Mote, and Stephen R. Spindler

Department of Biochemistry, University of California, Riverside.

Aging increases and caloric restriction (CR) decreases morbidity and mortality associated with the cardiovascular system. Using Affymetrix microarrays, we identified changes in heart gene expression induced by aging and CR in male mice. Eight weeks of CR (CR8) reproduced 19% of the long-term CR (LTCR)-related expression changes. Because CR8 begins to extend the life span of these mice, these genes may be keys to its cardioprotective effects. CR8 and LTCR changed gene expression in a manner consistent with reduced remodeling and fibrosis, and enhanced contractility and energy production via lipid β-oxidation. Molecular and histochemical studies indicated that CR reduced natriuretic peptide precursor type B and collagen expression, and reduced perivascular collagen deposition. We found smaller cardiomyocytes in the left ventricle of old-LTCR mice, suggesting reduced age-related cell death. Eight weeks of control feeding returned 97% of the LTCR-responsive genes to control expression levels. Thus, key CR-induced effects are rapidly responsive to diet, suggesting reduced caloric intake has rapid, positive effects on the heart.

HEART failure is the major cause of hospitalization, disability, and death in people more than 65 years old in the United States (1). Aging impairs cardiovascular capacity, contractility, and diastolic and systolic function (2). Aging is intimately associated with the development of diseases such as arterial hypertension and atherosclerosis. Each of these can modify myocardial structure and function. However, myocardial senescence remains poorly defined at the cellular and molecular level.

Mice are not generally used as models for cardiac aging. As a result, there is less known about cardiac changes with age in the mouse than is known in rats and humans. However, mice develop cardiomyopathy with age. For example, approximately 40% of male C57BL/6 mice develop cardiomyopathy by 1000 days of age (3). Accordingly, aging produces extensive changes in cardiac gene expression in mice [(4) and see below]. In rats and humans, three major age-associated changes markedly affect myocardial performance. First, myocardial fibrosis, a hallmark of cardiac aging in both humans and rats, is initiated by cellular necrosis and apoptosis (5,6). Cell death appears to induce reparative interstitial and perivascular collagen deposition, which plays a key role in the development of fibrosis in aged human and rodent hearts (7). Fibrosis decreases cardiac distensibility and increases diastolic pressure, impairing coronary hemodynamics and lowering coronary reserve (8,9). Second, the age-related decline in the number of cardiomyocytes with age is followed by compensatory myocyte hypertrophy (10,11). This remodeling leads to left ventricular hypertrophy, the most common cardiac manifestation of aging (12). Remodeling necessitates increased atrial and ventricular filling pressure. Third, age-related impairment in mitochondrial bioenergetics appears to contribute to myocardial stiffness, apoptosis, atrophy, and compensatory hypertrophy (13,14). Thus, these age-related changes to the heart appear to underlie age-related cardiac arrhythmias, dysfunction, and failure.

Caloric restriction (CR), undernutrition without malnutrition, is the most robust nutritional means of extending life span (15–17). We have shown that in older mice, CR begins within 2 months to reduce morbidity and mortality and to extend life span (15). CR is known to be a highly effective means of reducing the incidence and increasing the mean age of onset of cardiovascular diseases (18). However, there are few published studies of the effects of CR on the biochemistry or molecular biology of the heart. Further, we know of no studies of the transition of the heart to and from the CR state. Understanding the effects of initiating CR on the heart is crucial. Many of the pathologies and contributing factors associated with cardiovascular disease, such as diabetes, can be rapidly ameliorated by weight loss. However, the molecular mechanisms responsible for these effects are poorly understood. Here we report the microarray studies of the heart after shifts of old control mice to CR, and old CR mice to control feeding. We also report related molecular and immunohistochemical studies. These results show that the initiation and withdrawal of CR rapidly alters the expression of genes associated with myocardial fibrosis, tissue remodeling, and hemodynamic stress. We also report that long-term CR (LTCR) reduce perivascular collagen

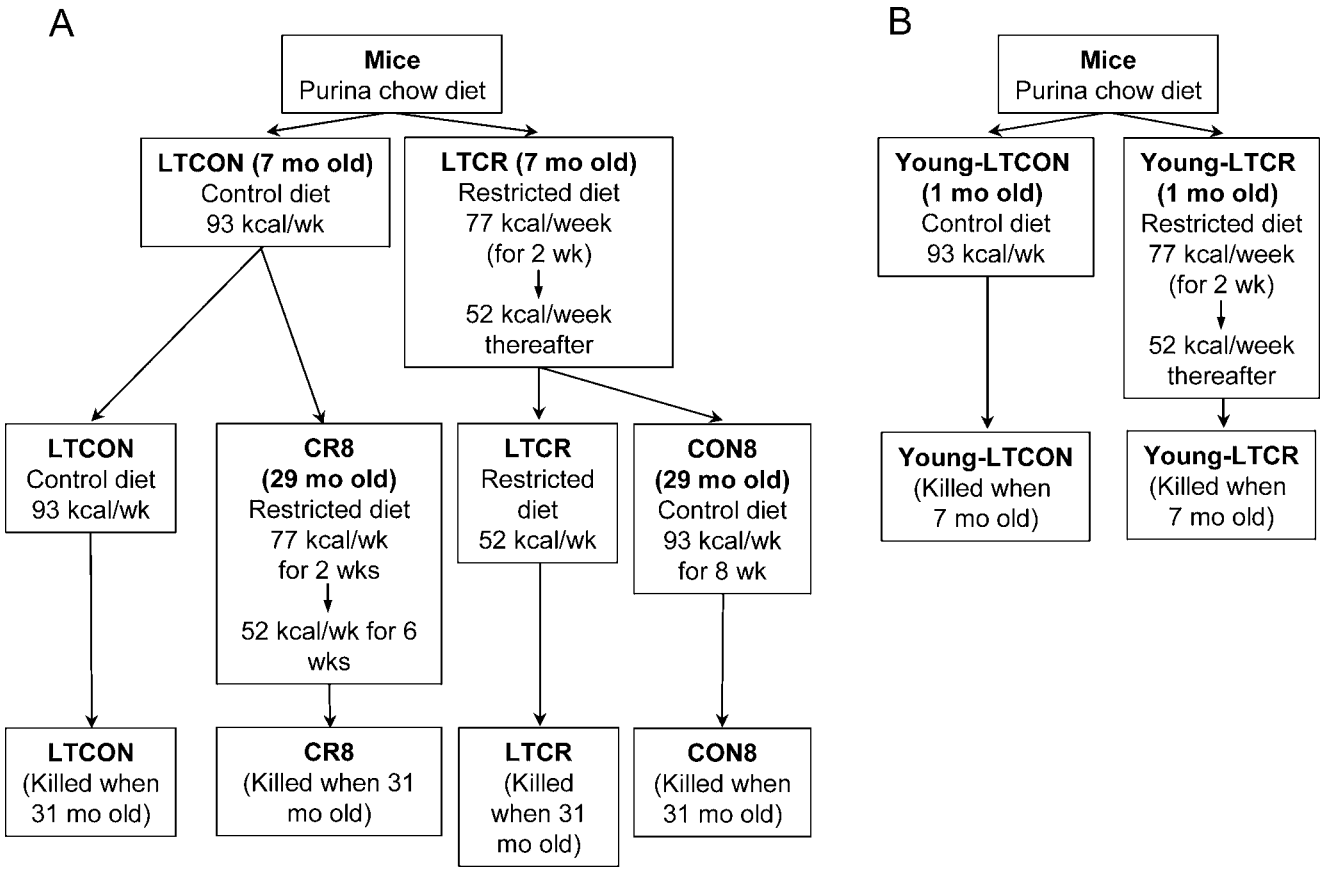

Figure 1. Study design. **A,** Mice were randomly assigned to one of two groups at 7 months of age, long-term control (LTCON) or long-term caloric restriction (LTCR). Cohorts of LTCR and LTCON mice were maintained on the diets. At 29 months of age, a cohort of LTCON mice were shifted to CR for 8 weeks (CR8), and a cohort of LTCR mice were shifted to control feeding for 8 weeks (CON8). All mice were killed at 31 months of age. **B,** Other cohorts of mice were shifted from a chow diet at 1 month of age to either a control or CR diet and killed at 7 months of age. See Methods for details.

deposition and maintained smaller and therefore physiologically younger cardiomyocytes in the left ventricle.

Methods

Study Design

Male B6C3F1 mice were fed mouse chow (PMI Nutrition International Product #5001; Purina Mills, Richmond, IN) and tap water ad libitum and maintained as described after weaning (19). Mice were randomly assigned to 4 groups at 7 months of age (Figure 1A). Long-term control (LTCON) mice were fed 93 kcal/week control diet (Diet No. F05312; BIO-SERV, Frenchtown, NJ). LTCR mice were fed 52.2 kcal/week of CR diet (Diet No. F05314; BIO-SERV). CR8 mice were maintained on control diet (93 kcal/week) from 7 to 29 months of age, and were transferred to a CR diet for 2 months before killing. The CR diet was introduced by feeding 77 kcal/week of CR diet for 2 weeks followed by feeding of 52.2 kcal/week thereafter. CON8 mice were a cohort of 29-month-old LTCR mice shifted to 93 kcal of control diet per week for 8 weeks. All the above mice were killed at 31 months of age. This protocol produced cohorts of old-LTCR, old-LTCON, old-CR8, and old-CON8 mice ($n = 4$).

A separate cohort of male B6C3F1 mice were fed mouse chow and tap water ad libitum after weaning, and were maintained as described (19). At 1 month of age, they were assigned to a young control group fed 93 kcal/week control diet (young-LTCON) or a young CR group (young-LTCR) fed 77 kcal of CR diet for 2 weeks and 52.2 kcal for 5.5 months (Figure 1B). Both groups were 7 months old when killed by cervical dislocation. All mice were fasted 48 hours before killing ($n = 4$).

Mouse weights at death were: young-LTCR, 26.65 $\pm$ 0.71 g (standard deviation); young-LTCON, 41.35 $\pm$ 0.66 g; old-LTCR, 22.1 $\pm$ 2.6 g; old-LTCON, 34.7 $\pm$ 4.4 g; CR8, 29.3 $\pm$ 2.8 g; CON8, 29.2 g $\pm$ 1.8 g. Hearts were excised rapidly, rinsed in phosphate-buffered saline, examined for signs of pathology, and flash frozen in liquid nitrogen. The other organs were examined visually for signs of pathology. No pathology was detected in the animals used. All animal use protocols were approved by the Institutional Animal Use Committee of the University of California, Riverside.

Microarray Measurement of Gene Expression

Heart total RNA was isolated as described (20). Copy RNA (cRNA) hybridization intensity for each mouse was

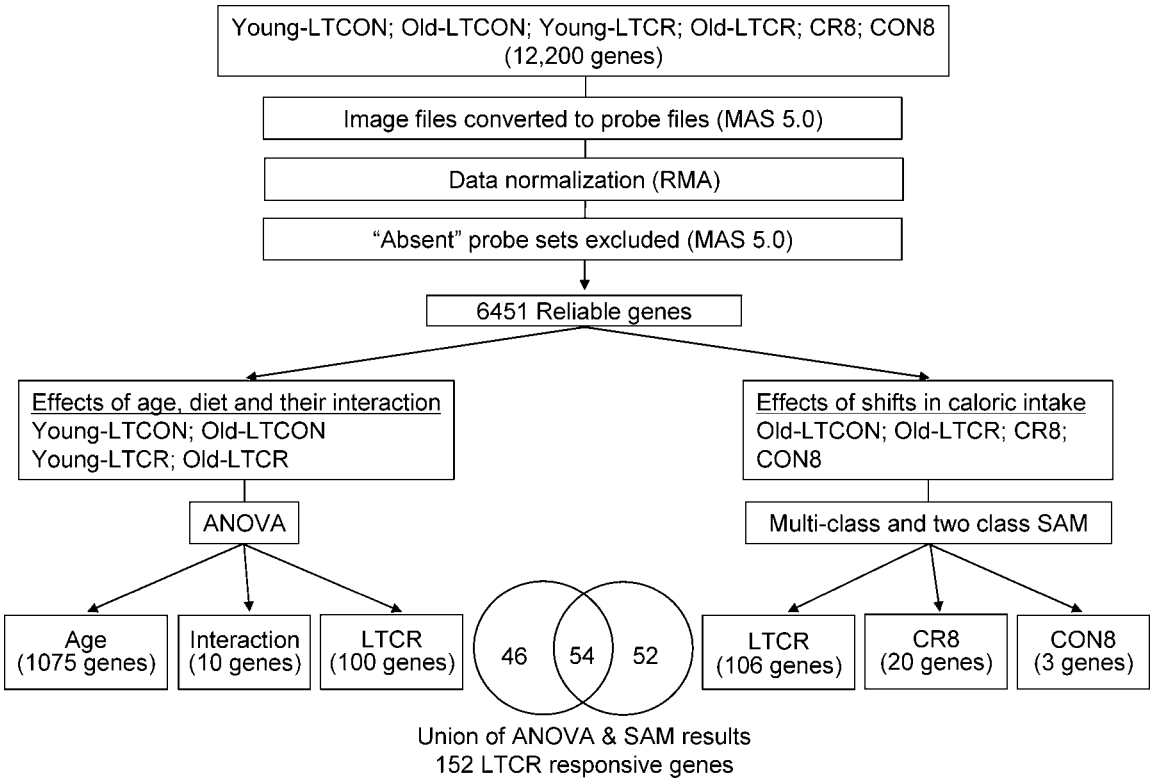

Figure 2. Data normalization and analysis. Affymetrix data were normalized and the data reduced using Microarray Suite (MAS) 5.0 and Robust Multichip Average (RMA). After normalization and data reduction, data from the young- and old-long-term caloric restriction (LTCR) and control groups were examined using analysis of variance (ANOVA) to determine the effects of age, diet, and their interaction. The normalized reduced data were also subjected to multiclass Significant Analyses for Microarray (SAM), followed by a two-class unpaired SAM to determine the effects of dietary shifts. These analyses produced two intersecting sets of genes changed in expression by LTCR (Venn diagram). The number of genes in each set is shown in parenthesis. LTCON = long-term control; CR8 = 8 weeks of CR; CON8 = LTCR mice shifted to control feeding for 8 weeks.

measured using an Affymetrix mouse U74Av2 array according to standard Affymetrix protocols (Affymetrix, Santa Clara, CA; 19). One array was used for heart RNA purified from each of 24 mice, 4 mice from each experimental group (old-LTCR, old-LTCON, old-CR8, old-CON8, young-LTCR, and young-LTCON).

Data Analysis

Image analysis was performed as described (19). Image files were converted to probe set data (*.CEL files) using Microarray Suite (MAS 5.0; Figure 2). Probe set data from all 24 arrays were analyzed simultaneously with the Robust Multichip Average method to generate normalized expression measures for each probe set (21). The data were further filtered to exclude probe data sets that were ''Absent'' across all 24 arrays according to the MAS 5.0 Wilcoxon signed rank test (22). There were 6451 genes which passed these criteria. All gene names were obtained from the LocusLink and/or Affymetrix databases as of August 2005.

Using data from young-LTCON, young-LTCR, old-LTCON, and old-LTCR mice, we performed two-way analysis of variance (ANOVA) in which mRNA levels were considered to be a function of age only, diet only, or both age and diet (Figure 2). We used a parametric test that assumed equal variance and a multiple testing correction based on the Benjamini and Hochberg False Discovery Rate (GeneSpring 6.1; Silicon Genetics, Redwood, CA). The ANOVA was based on the model: $y_{ijk} = \mu + A_i + D_j + (A \times D)_{ij} + \varepsilon_{ijk}$, where μ is the overall mean intensity value of gene expression that is common to all samples; A_i is the effect of the i^{th} age (young and old); D_j is the effect of the j^{th} diet (CON and LTCR); $(A \times D)_{ij}$ is the interaction between age and diet; and ε_{ijk} is the stochastic error. The term y_{ijk} represents the observed value of gene expression for the k^{th} replicate of the i^{th} age under j^{th} diet. An interaction between age and diet would indicate that the effect of diet on gene expression is conditional on age. The fold change was calculated as follows: For an age only effect ($A_i \neq 0$, $D_j = 0$, $(A \times D)_j = 0$), the fold change of old versus young was estimated by $2^{|A1-A2|}$ for an upregulated gene (or $-2^{|A1-A2|}$ for a downregulated gene). This estimation was based on (old-LTCR + old-LTCON) versus (young-LTCON + young-LTCR) because diet does not have an effect ($D_j = 0$) and there is no interaction between age and diet ($(A \times D)_j = 0$). For genes affected only by diet ($D_j \neq 0$, $A_i = 0$, $(A \times D)_j = 0$), the fold change of LTCR versus CON was estimated by $2^{|D1-D2|}$ (or $-2^{|D1-D2|}$). The estimation of fold change was based on (young-LTCR + old-LTCR) versus (young-LTCON + old-LTCON) because age does not affect these genes ($A_i = 0$) and there is no interaction between age and diet ($(A \times D)_j = 0$). When both age and diet affect gene expression but with no interaction ($D_j \neq 0$, $A_i \neq 0$, $(A \times D)_j = 0$), the fold change is

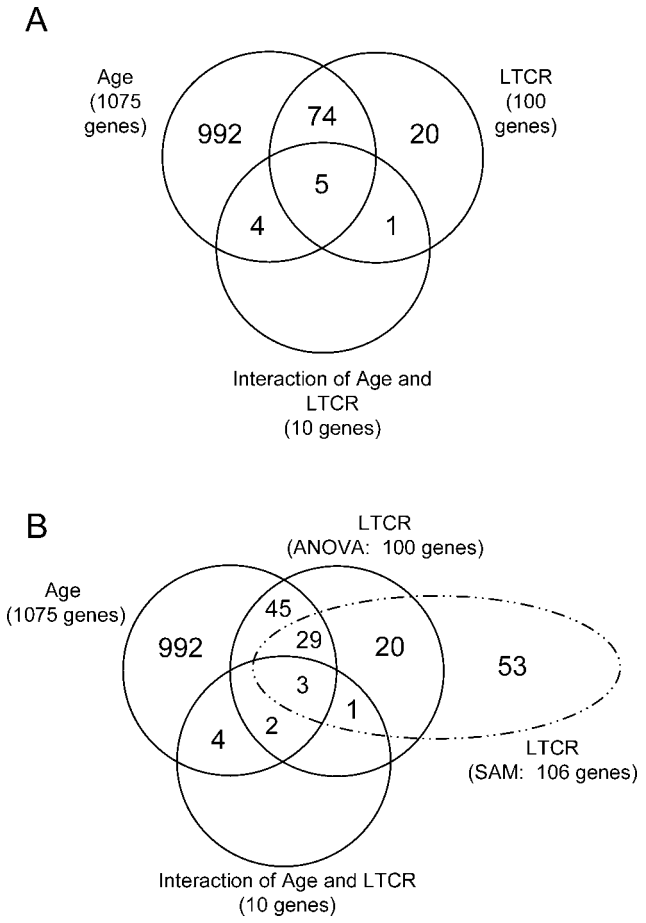

Figure 3. Venn diagrams of the gene sets obtained from the statistical analysis. **A,** Effects of age, diet, and their interaction determined by analysis of variance (ANOVA). Nine hundred ninety-two genes were affected only by age, 20 genes only by long-term caloric restriction (LTCR), and 74 genes independently by age and CR. There was evidence of an interaction between age and diet for only 10 genes. **B,** Intersection of the 100 LTCR-responsive genes found by ANOVA (*solid circles*) and the 106 found by Significant Analyses for Microarray (*dot-dashed circle*) was 53 genes. Of these genes, most were independently affected by age and diet (49 genes).

estimated by $2^{|D1-D2+A1-A2|}$ (or $-2^{|D1-D2+A1-A2|}$). This estimation has to be based on young-LTCON versus old-LTCR, otherwise we can not detect the combined effect of both age and LTCR. When there is an interaction between the effects of diet and age (we identified only nine such genes in our study), the fold change resulting from the interaction has to be based on old-LTCR versus young-LTCON and is estimated by $2^{|D1-D2+A1-A2+(D\times A)11-(D\times A)22|}$ (or $-2^{|D1-D2+A1-A2+(D\times A)11-(D\times A)22|}$). However, if we want to know the effect of age on these nine genes we must use the old-LTCON versus young-LTCON and not (old-LTCR + old-LTCON) versus (young-LTCON + young-LTCR) because of the interaction. Similarly, the effect of LTCR in old (or in young) for the nine genes is estimated from old-LTCR versus old-LTCON (or young-LTCR vs young-LTCON).

To resolve the effects of dietary shifts on gene expression, normalized and filtered data from the old-LTCON, old-LTCR, CR8, and CON8 groups were subjected to multiclass Significant Analyses for Microarray (SAM; 23). We used a median False Discovery Rate of less than 5.0%. To identify differentially expressed genes, the output also was subjected to two-class unpaired SAM. This is a nonparametric analysis.

Microarray Data Validation

Nine of the genes that changed expression with LTCR according to both the ANOVA and SAM were re-examined by real-time, two-step reverse transcription-polymerase chain reaction (qPCR) using a QuantiTect SYBR Green PCR kit (Qiagen, Hilden, Germany) and an ABI PRISM 7700 Sequence Detection System (Applied Biosystems, Foster City, CA). Primers were designed using the Netaffx analysis center, and PCR products were sequenced and verified against the public database. Primer sequences are shown in Supplementary Table 1. **[Supplementary Tables are linked to the online article in the March issue at *http://biomed.gerontologyjournals.org/content/vol61/issue3/*.]** Primers for transcription elongation factor A (SII) 1 were amplified in parallel with the gene of interest as a control. This mRNA is unaffected by CR in the heart relative to total polyadenylated RNA or ribosomal RNA abundance (data not shown). Amplification specificity was confirmed by melting curve analysis and agarose gel electrophoresis.

Western Blot Analysis

Protein (~25 mg) was extracted from the tip of the left ventricle as described (24). Aliquots (15 μg) were separated on 6% sodium dodecyl sulfate–polyacrylamide gels, transferred to polyvinylidene fluoride membranes (Millipore, Billerica, MA), stained with Ponceau S for data normalization, and incubated for 2 hours with primary rabbit anti-collagen types I or III antibody (Rockland Labs, Gilbertsville, PA). Washed blots were incubated for 1 hour with horseradish peroxidase-labeled goat anti-rabbit immunoglobulin G (Santa Cruz Biotechnology, Santa Cruz, CA), and bands were detected with an enhanced chemiluminescence (ECL) kit (Amersham Biosciences, Piscataway, NJ).

Histology and Immunohistochemistry

Ring sections (5 μm) of myocardial tissue were fixed in Bouin's solution, paraffin embedded, and sectioned using standard techniques. Sections were stained with 0.1% Sirius red F3BA (Aldrich Chemical Co, Milwaukee, WI) as described (25). Nuclei were counterstained with hematoxylin. Collagen types were resolved with Polaroid filters (26). Antigen retrieval was performed with 0.1% pepsin in 0.5 M acetic acid. Sections were layered with either rabbit anti-collagen types I or III (Rockland Laboratories), or control normal rabbit immunoglobulin (Dako, Carpinteria, CA) and visualized with a Vectastain Elite ABC kit (Vector Laboratories, Burlingame, CA). The average cross-sectional area of cardiomyocytes from LTCR and LTCON mice was quantified in arbitrary units by printing digital images of the cardiomyocytes from individuals in each group at identical magnifications, cutting out cell images from each print, weighing the cutouts, and averaging the weights. The statistical significance of the difference in the weights

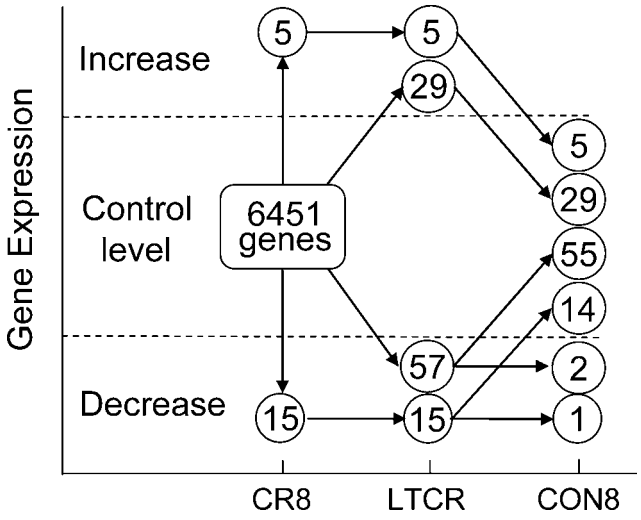

Figure 4. Effects of dietary shifts on long-term caloric restriction (LTCR)-responsive genes in the heart. Of the 6451 Robust Multichip Average and Microarray Suite filtered genes, 106 LTCR-responsive genes were found using Significant Analyses for Microarray analysis. Shown is the effect of LTCR, 8 weeks of CR (CR8), and shifting LTCR mice to control feeding for 8 weeks (CON8) on the expression of these genes.

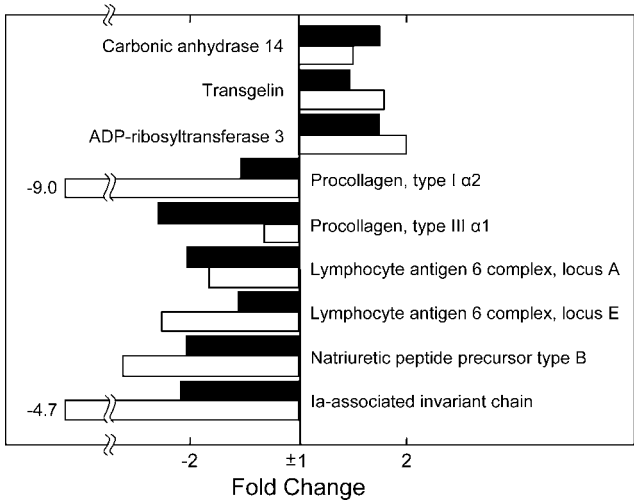

Figure 5. Microarray and real-time, two-step reverse transcription-polymerase chain reaction using a QuantiTect SYBR Green PCR kit (qPCR) quantitation of nine genes. *Solid bars*, means of messenger RNA levels in long-term calorie-restriced (LTCR) mice divided by the means of the levels in long-term control (LTCON) mice, as determined by qPCR. *Open bars* reflect the Significant Analyses for Microarray (SAM) of the data. *Solid bars*, means of mRNA expressed in LTCR mice ($n = 4$) divided by the means in LTCON mice ($n = 4$) as determined by qPCR. The expression of each gene (± standard error) as determined by qPCR, in control and LTCR mice, was (in arbitrary units): procollagen, type I α2, 1.04 ± 0.12 and 0.67 ± 0.15; procollagen, type III α1, 2.01 ± 0.19 and 0.86 ± 0.25; carbonic anhydrase 14, 0.94 ± 0.06 and 1.65 ± 0.09; transgelin, 1.32 ± 0.10 and 1.90 ± 0.19; adenosine diphosphateribosyltransferase 3, 0.63 ± 0.03 and 0.94 ± 0.05; lymphocyte antigen 6 complex, locus A, 1.24 ± 0.23 and 0.60 ± 0.08; lymphocyte antigen 6 complex, locus E, 1.08 ± 0.07 and 0.70 ± 0.15; natriuretic peptide precursor type B, 1.56 ± 0.15 and 0.75 ± 0.17; Ia-associated invariant chain, 0.65 ± 0.10 and 1.41 ± 0.04.

between the groups was determined using a two-sample *t* test ($n = 10$ cell images per group).

Results and Discussion

Effects of Age, LTCR, and Their Interaction on Gene Expression

Six statistical categories of expressed genes were identified using two-way ANOVA (Figure 2, left side; Figure 3A). Of these, 1075 genes changed expression with age and 100 genes changed expression with LTCR (Supplementary Tables 2–7). Seventy-four genes were affected independently by age and diet (Figure 3A; Supplementary Table 3). LTCR reversed the age-related change in the expression of 47 of these 74 genes (Supplementary Table 3). Twenty genes changed expression only with LTCR (Figure 3A; Supplementary Table 4). The effects of CR were dependent on age for five genes (Figure 3A; Supplementary Table 5). Thus, LTCR affected the expression of only 79 of the 1075 age-responsive genes (74 plus 5; Figure 3A).

The effects of LTCR on cardiac gene expression were largely age-independent (Figure 3; Supplementary Tables 5–7). The heart genes which were LTCR-responsive in young mice were a subset of the heart genes that were LTCR responsive in old mice. Because CR appears to be equally effective regardless of age, these genes may be key to its health and longevity effects (15,16).

Effects of Shifts in Caloric Intake on Gene Expression

Effects of short-term CR on gene expression.—SAM identified 106 LTCR-responsive genes (Figures 2 right side, 3B, and 4; Table 2). Twenty of these genes changed expression after only 8 weeks of CR (19%; Figure 4; Table 2). Because CR8 begins to extend the life span of mice and delay the onset of age-related diseases, the gene expression changes induced by CR8 may be most germane to the cardioprotective benefits of CR (15).

Dissipation of the effects of LTCR.—Shifting LTCR mice to control feeding for 8 weeks (CON8) returned 103 of the 106 LTCR-responsive transcripts to control expression levels (97%; Figure 4, Table 2). These results are similar to those found in liver, suggesting that most LTCR-responsive genes can react rapidly to diet (15). Shifts to and from CR in *Drosophila* result in rapid changes in the short-term risk of death (16). Thus, rapid mechanisms of life-span extension exist in at least two widely divergent species.

Comparison of LTCR-Responsive Genes Determined by ANOVA and SAM

ANOVA and SAM identified overlapping sets of LTCR-responsive genes (Figure 2, center bottom; Figure 3B). The identification of such nonidentical, overlapping sets is common when different methods of data analysis are used (27). ANOVA and SAM produce nonidentical lists in part because they measure different parameters, make different

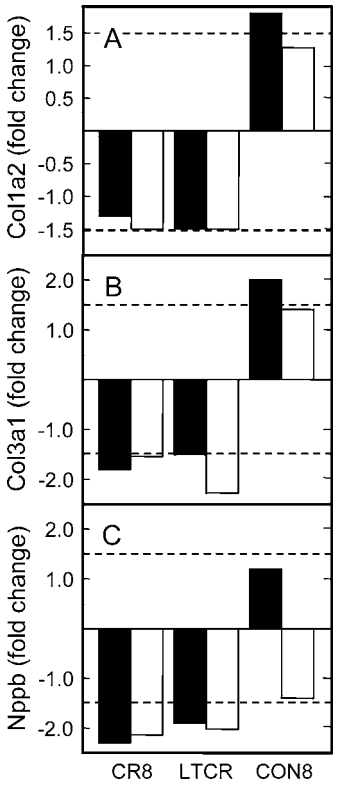

Figure 6. Quantification of procollagen, type I, α2 (Col1a2; **A**), procollagen, type III, α1 (Col3a1; **B**), and natriuretic peptide precursor type B (Nppb; **C**) expression by microarrays and real-time, two-step reverse transcription-polymerase chain reaction using a QuantiTect SYBR Green PCR kit (qPCR). *Solid bars*, ratios of the means measured by qPCR. *Open bars*, fold change from the microarray data analysis. CR8 = 8 weeks of caloric restriction; LTCR = long-term CR; CON8 = LTCR mice shifted to control feeding for 8 weeks.

assumptions about the underlying data, and use different subsets of the data to generate the gene lists. Both analyses appear to have identified authentically changed genes. We confirmed the changes in gene expression of nine found genes in both sets using qPCR (Figure 5).

Functional Classification of CR-Responsive Genes

Consistent with the ability of LTCR and short-term CR to ameliorate risk factors associated with cardiac aging (28,29), CR had major effects on genes associated with fibrosis and tissue remodeling, in addition to other key physiological aspects of aging. These included reduced expression of genes with key roles in extracellular matrix and cytoskeletal structure and dynamics, cell motility, inflammation, increased peroxisome proliferator-activated receptor α (PPARα) signal transduction, and fatty acid metabolism (Table 2). We will discuss these changes further below.

Fibrosis and Ventricular Remodeling

Myocardial collagen and extracellular matrix expression and accumulation increase with age, contributing to increased fibrosis, myocardial stiffness, diastolic pressure, and heart failure. We detected gene expression, molecular, and immunohistochemical changes in CR mice consistent with reduced cardiac fibrosis and remodeling. LTCR and CR8 inhibited the expression of the collagen genes Col1a1 (procollagen, type I, α1), Col1a2 (procollagen, type I, α2), Col3a1 (procollagen, type III, α1), and Col5a1 (procollagen, type V, α1; Table 2). Col6a3 (procollagen, type VI, α3) expression also was reduced by LTCR. We confirmed the decrease in the expression of Col1a2 and Col3a1 in LTCR and CR8 mice by using qPCR (Figures 5 and 6). Using western blots of protein extracted from left ventricles of old mice, we found that LTCR reduced steady-state collagen I and III protein levels in the left ventricle of old mice by ~50% (Figure 7). Histochemical staining with Picrosirius red revealed that perivascular collagen deposition was much reduced in the left ventricle of old mice (Figure 8, A and B). Using polarization microscopy to resolve types I and III collagen, we found that deposition of both collagen types was reduced (Figure 8, C and D).

Perivascular collagen is primarily type I, which is less distensible than type III. For this reason, reduced deposition of type I collagen in the perivascular space of CR mice is consistent with greater elasticity and less perivascular fibrosis. In addition, LTCR, and in most cases CR8, reduced transcripts for other key extracellular matrix and cell-adhesion-related proteins (Cpxm2, Tnxb, Crtap, Lgals1, Fbn1, and Ifitm3; Table 2). These changes suggest that CR reduced the expression and deposition of many adhesion and extracellular matrix proteins. As discussed above, these effects should lead to reduced cardiac stiffness, cardiac and perivascular fibrosis, and hemodynamic stress.

Vascular wall stress stimulates interstitial fibroblasts to secrete collagen and other extracellular components. Thus, by directly preventing the overexpression of these genes, CR should reduce hemodynamic stress. CR also may reduce hemodynamic stress by reducing the expression of atrial natriuretic peptide precursor type B (Nppb; Table 2). Nppb has diuretic, natriuretic, and vasodilatory activities. This hormone, which is produced mainly by the ventricles, is a sensitive and specific marker of ventricular pathology (30). Nppb expression increases with congestive heart failure in animal models and humans (31,32). Aging increased murine Nppb expression, extending results found for rats (Table 1) (33). LTCR and CR8 decreased Nppb expression (Table 2; Figure 6). This finding suggests that CR acts in at least two ways to reduce cardiac fibrosis, cardiomyocyte loss, and tissue remodeling—by inhibiting both extracellular matrix and Nppb expression.

LTCR and in some instances CR8 also downregulated the transcripts for Prkwnk1 (also called Wnk1), Dscr1 (calcipressin 1), and Serpina3n (Table 2). Together these effects are consistent with rapidly reduced blood pressure in CR mice. Mutations in the Prkwnk1 protein kinase which increase its expression are implicated in a familial form of hypertension (34). Mutational inactivation of Dscr1, a protein phosphatase, decreases stress-induced cardiac hypertrophy. Serpina3n inhibits neutrophil cathepsin G and mast-cell chymase, which convert angiotensin I to II, resulting in vasoconstriction, fluid retention, and increased blood pressure. The rapid response of the genes discussed above to CR8 is accordant with the effects of low-calorie diets on blood pressure in monkeys and humans (29,35,36).

In accord with the interpretation of the expression data

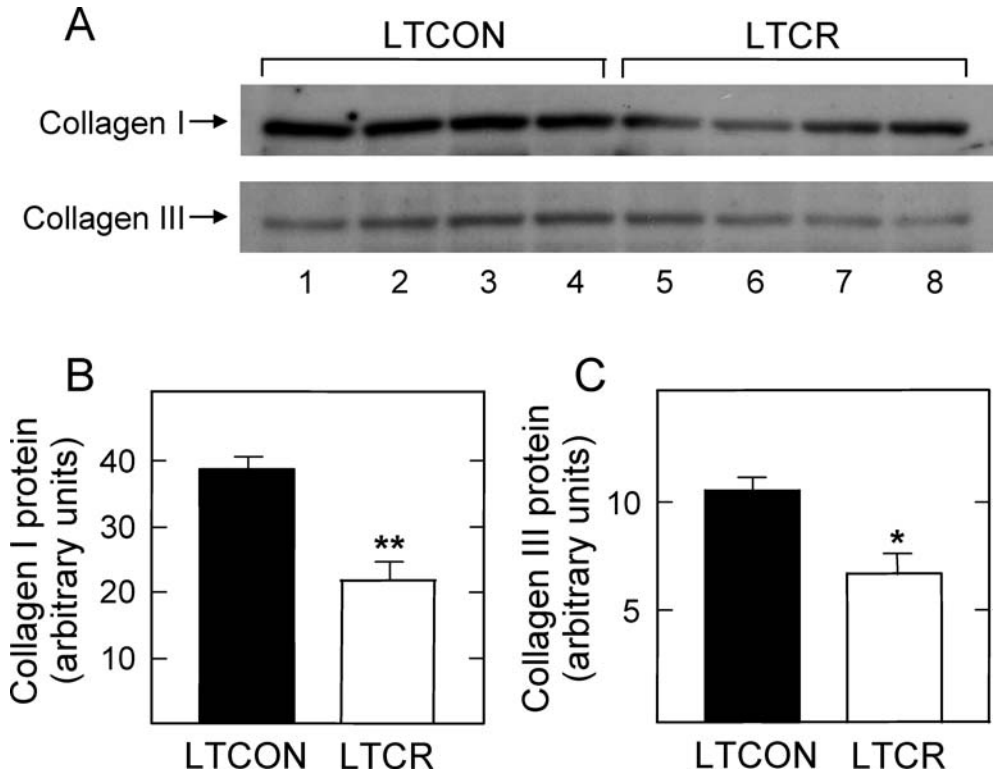

Figure 7. Collagen I and III protein levels in the left ventricle of hearts. **A,** Western blots of total protein from long-term control (LTCON) mice (*lanes 1–4*) and long-term caloric restriction (LTCR) mice (*lanes 5–8*). **B** and **C,** Densitometric quantification of collagen type I and type III protein levels from the blots shown in A. Data were normalized using Ponceau S staining. The data are the means ± standard error of the mean. The difference in protein levels was significant (*$p < .05$, **$p < .01$).

described above, cardiomyocytes on the outer part of the left ventricular wall of LTCR mice were smaller than those from control mice (Figure 8E and F). The cross-sectional area of cardiomyocytes from LTCON mice (59.5 ± 10.2 arbitrary units) was on average 1.8-fold larger than that of LTCR mice (33.9 ± 12.8 arbitrary units; $p < .001$). The number of cardiomyocytes declines significantly with age in both rats and humans (10). During aging, myocyte death from hemodynamic stress leads to myocardial atrophy, followed by compensatory hypertrophy of the remaining cardiac myocytes. These changes result in the accumulation of larger, older cardiomyocytes. These older cells respond poorly to growth stimuli, and undergo higher rates of necrosis and apoptosis. Thus, the presence of smaller cardiomyocytes in LTCR mice is consistent with the maintenance of functionally younger, healthier cardiomyocytes (37). This result is consistent with the reduced tissue remodeling in LTCR mice.

Enhanced cytoskeletal dynamics and nonmyocyte cell division are also key features of ventricular remodeling. LTCR and in some instances CR8 increased the expression of the antiproliferation-associated genes Cdkn1a (cyclin-dependent kinase inhibitor 1A; also called Waf1/p21Cip1), the expression of which is associated with p53-induced cell cycle arrest in cardiomyocytes; Sesn1 (sestrin 1), a growth arrest inducible, p53 binding protein; Btg3, which induces growth arrest by indirectly stabilizing p53; and Ndrg4 (also called Smap8), which reduces the proliferation and migration of aortic smooth muscle cells. LTCR and CR8 decreased the expression of the proliferation-associated genes Mapk1 (mitogen-activated protein kinase 1, also called ERK), which activates growth-related transcription factors, leading to cardiac hypertrophy; and Rps6ka2, which is a terminal kinase in the Mapk1 pathway which phosphorylates ribosomal protein S6, and thereby enhances the translation of cell-growth and division-related mRNA. Elevated expression of this gene is linked to cardiovascular disease (38,39). Together, these results suggest that CR increases antiproliferative (and decreases proliferative) gene expression in the heart, reducing remodeling.

LTCR and in some instances CR8 also downregulated eight genes involved in cytoskeleton organization and structure (Ly6a [ataxin-1], Ly6e, Ptmb4 [thymosin β4], Tmsb10 [thymosin, β10], Pfn2 [profilin 2]; Sept4, Gsn [gelsolin], and Marcks). Together, these results also are consistent with reduced ventricular remodeling in LTCR and CR8 mice.

Signal Transduction

Age-related impairment in mitochondrial energy generation may contribute to age-related myocardial stiffness, apoptosis, atrophy, and compensatory hypertrophy. Because myocardial energy reserves are limited, a constant supply of high-energy phosphates is required (13). β-oxidation of fatty acids provides 40%–50% of the acetyl-coenzyme A (CoA) produced by the heart (40). However, the capacity for fatty

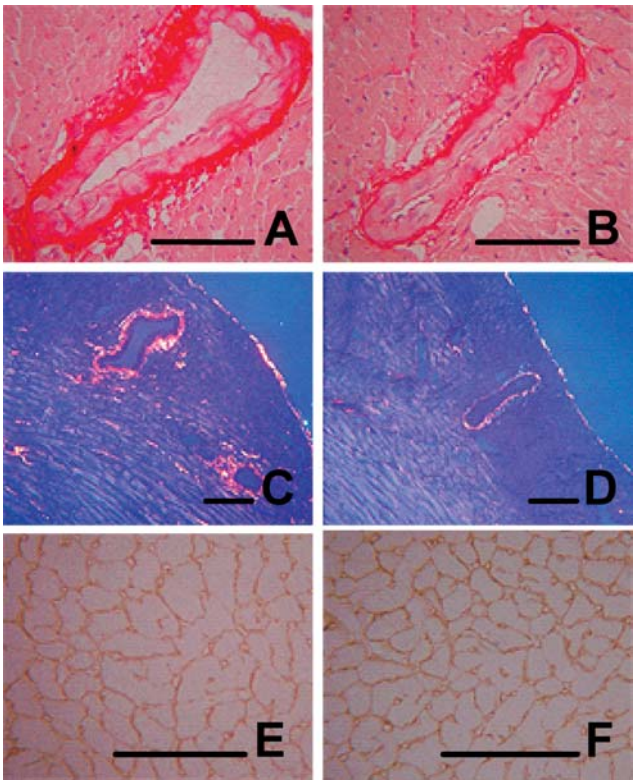

Figure 8. Photomicrographs of collagen deposition in the left ventricle of control (**A, C,** and **E**) and long-term caloric restriction (LTCR) (**B, D,** and **F**) mice. A and B, Picrosirius-red stained mouse left ventricular tissue sections showing perivascular collagen deposits. C and D, Polarized microscopy showing perivascular collagen I and III deposits. Collagen I is stained yellow, orange, or red; collagen type III appears greenish (26). E and F, Left ventricular cardiomyocytes immunohistochemically stained for collagen I. Scale bars are 100 μm.

acid oxidation is reduced by aging (41,42). PPARα is a lipid-activated transcription factor which regulates the expression of many of the key genes mediating fatty acid β-oxidation. It is thereby a key regulator of energy homeostasis in the heart (14). Levels of PPARα are reduced in the heart during aging (42). Decreased PPARα expression is a likely cause of reduced fatty acid utilization during hypertrophy in failing human hearts (43). We found that LTCR upregulated PPARα and decreased rev-erbAα transcripts. Rev-erbAα antagonizes transactivation by PPARα (44). Thus, PPARα expression and activity are likely upregulated in the heart by CR, suggesting that CR acts directly at the level of transcription to enhance fatty acid β-oxidation.

Concordant with this result, LTCR increased the expression of two genes which are upregulated by PPARα signaling in the heart, Lp1 (lipoprotein lipase) and Cte1 (a cytosolic acyl-CoA thioesterase; 45,46). Lipoprotein lipase liberates free fatty acids from circulating triglyceride-rich lipoproteins, which are considered a principal energy source for the heart. Cte1 catalyzes the hydrolysis of acyl-CoA thioesters to free fatty acids and CoA.

CR altered the expression of other cardioprotective signal transduction systems. LTCR upregulated Adcy6, an adenylate cyclase preferentially expressed in cardiac myocytes. LTCR negatively regulated Pkia (protein kinase inhibitor α), an inhibitor of cyclic adenosine monophosphate-dependent protein kinase A. Adcy6 overexpression enhances left ventricular contractile function, and improves survival in murine cardiomyopathy (47,48). Increased intracellular cyclic adenosine monophosphate levels activate protein kinase A, leading to enhanced cardiac contractility. LTCR and CR8 also downregulated Gprk5, major cardiomyocyte G protein-coupled receptor kinase, overexpression of which impairs myocardial function and is associated with hypertension and postinfarction failure (49).

Immune Response and Inflammation

PPARα agonists reduce inflammation and the formation of atherosclerotic lesions, even in the absence of their lipoprotein-lowering effects (14,50,51). In accord with its enhancement of PPARα expression, LTCR negatively regulated the expression of inflammation-related genes (C1qb, C1qg, Serping1, H2-Aa, H2-K2, Klra9, and Ii). It also reduced the expression of at least six interferon-inducible genes (Ifitm3, Ifi205, Ifi16, H2-Aa, H2-K2, and Ii), suggesting reduced interferon levels. Downregulation of these genes is consistent with the systemic decrease in inflammation observed in CR rodents. Reduced systemic inflammation may be the source of the decreased cardiovascular disease found in CR animals and humans (29).

Age Effects on Gene Expression

Aging was accompanied by the overexpression of genes associated with impaired cardiac function and cardiovascular disease. Aging increased the expression of genes encoding sarcomeric (Myh7, Myl2, and Mybpc3) and cytoskeletal (Actb and Cfl1) proteins (Table 1). Cardiac hypertrophy is associated with overexpression of sarcomeric proteins (52). Aging decreased the expression of Itgb1 and Timp3, and increased the expression of Bgn. These genes are keys to remodeling of the collagen matrix. Disregulation of matrix remodeling is a causal factor in heart failure (53).

Aging decreased the expression of a mix of positive (Fgf1, Vegfa, Tek, Kitl, Sept7, Orc4l, and Mtm1; Table 1) and negative (Gas5, Tob1, Ppp1cb, and Ccng1) regulators of cell division and growth, and altered the expression of a mix of proapoptotic (Pdcd8 and Bnip3l) and antiapoptotic (Bag1, Atp6v1g1, and Atp6v1c1) factors. These effects support the observation that the aging myocardium is a site of both myocyte death and cell division (54).

Aging also altered the expression of genes involved in histone acetylation and deacetylation (Hdac2, Chd4, Mxi1, Morf412, Cited2, Cri1, and Pcaf; Table 1). The importance of Sir2, a histone deacetylase, in the replicative life span of yeast and life span of nematodes suggests that these effects may be significant (55). Aging decreased the expression of 12 genes of the ubiquitin–proteasome system, possibly indicating decreased protein turnover in older myocytes (Table 1).

Similarities of Our Results to Those in Other Reports

A recent microarray study (56) found gene expression changes consistent with preserved fatty acid metabolism, reduced DNA damage, decreased immune activity, modulation of apoptosis, and reorganization of the cytoskeleton.

Table 1. Selected Effects of Aging on Heart Gene Expression

GenBank	Gene	Description	Age FC*	p Value†
Signal transduction and growth factors				
L49507	Ccng1	Cyclin G1	−2.8	1.5×10^{-8}
X71426	Tek	Endothelial-specific receptor tyrosine kinase	−2.9	1.3×10^{-11}
M30641	Fgf1	Fibroblast growth factor 1	−1.8	2.5×10^{-7}
AI849615	Gas5	Growth arrest specific 5	−1.9	3.7×10^{-7}
M57647	Kitl	Kit ligand	−2.2	6.1×10^{-9}
AI553463	Orc4l	Origin recognition complex, subunit 4-like (*Saccharomyces cervisiae*)	−2.7	9.0×10^{-10}
M27073	Ppp1cb	Protein phosphatase 1, catalytic subunit, beta isoform	−3.5	1.2×10^{-7}
AJ223782	Sept7	Septin 7	−2.2	3.4×10^{-9}
D78382	Tob1	Transducer of ErbB	−2.1	6.1×10^{-9}
M95200	Vegfa	Vascular endothelial growth factor A	−1.9	1.7×10^{-6}
AF073996	Mtm1	X-linked myotubular myopathy gene 1	−1.9	1.2×10^{-8}
Apoptotic factors				
AW121246	Atp6v1g1	ATPase, H^+ transporting, V1 subunit G isoform 1	−2.1	9.2×10^{-8}
U13839	Atp6v1c1	ATPase, H^+ transporting, V1 subunit C isoform 1	−2.1	1.0×10^{-7}
AF067395	Bnip3l	BCL/adenovirus E1B 19kd-interacting protein 3-like	−2.0	1.4×10^{-6}
AF022223	Bag1	Bcl2-associated athanogene 1	−2.1	6.0×10^{-9}
AF100927	Pdcd8	Programmed cell death 8	−2.0	2.9×10^{-7}
Extracellular matrix and cytoskeleton				
J04181	Actb	Actin, beta, cytoplasmic	2.5	1.3×10^{-9}
X53928	Bgn	Biglycan	2.3	4.6×10^{-8}
D00472	Cfl1	Cofilin 1, nonmuscle	2.5	5.9×10^{-13}
X15202	Itgb1	Integrin beta (fibronectin receptor beta)	−2.3	2.5×10^{-8}
AF059576	Mybpc3	Myosin binding protein C, cardiac	2.6	4.0×10^{-3}
M91602	Myl2	Myosin, light polypeptide 2, regulatory, cardiac, slow	2.1	3.5×10^{-11}
AJ223362	Myh7	Myosin, heavy polypeptide 7, cardiac muscle, beta	2.1	2.0×10^{-3}
U26437	Timp3	Tissue inhibitor of metalloproteinase 3	−2.1	2.0×10^{-8}
Histone acetylation and deacetylation				
Y15163	Cited2	Cbp/p300-interacting transactivator, with Glu/Asp-rich carboxy-terminal domain, 2	−2.1	9.9×10^{-6}
R75450	Chd4	Chromodomain helicase DNA binding protein 4	2.2	1.3×10^{-9}
AI844939	Cri1	CREBBP/EP300 inhibitory protein 1	−2.5	3.1×10^{-8}
U31758	Hdac2	Histone deacetylase 2	−2.0	5.8×10^{-9}
L38822	Mxi1	Max interacting protein 1	−2.2	5.1×10^{-7}
AA529583	Morf4l2	Mortality factor 4 like 2	−2.8	3.1×10^{-8}
D16497	Nppb	Natriuretic peptide precursor type B	2.5	1.4×10^{-8}
AW047728	Pcaf	p300/CBP-associated factor	−1.9	5.5×10^{-9}
Ubiquitin and proteasome				
AI839371	Psmc2	Proteasome (prosome, macropain) 26S subunit, ATPase, 2	−2.1	4.5×10^{-9}
AI836423	Psmc6	Proteasome (prosome, macropain) 26S subunit, ATPase, 6	−2.3	2.1×10^{-9}
AW121693	Psmd11	Proteasome (prosome, macropain) 26S subunit, non-ATPase, 11	−1.7	1.4×10^{-6}
Y13071	Psmd14	Proteasome (prosome, macropain) subunit, non-ATPase, 14	−1.5	5.1×10^{-6}
AA867340	Psme4	Proteasome (prosome, macropain) activator subunit 4	−1.9	9.9×10^{-9}
AF055983	Psma3	Proteasome (prosome, macropain) subunit, alpha type 3	−2.1	8.7×10^{-9}
AB003304	Psmb5	Proteasome (prosome, macropain) subunit, beta type 5	−2.4	6.8×10^{-9}
AW060186	Usp14	Ubiquitin-dependent protein catabolism synaptic transmission	−2.1	1.8×10^{-6}
AW124623	Ube2g1	Ubiquitin-conjugating enzyme E2G 1 (UBC7 homolog, *Caenorhabditis elegans*)	−1.9	6.1×10^{-9}
AW210080	Ube2n	Ubiquitin-conjugating enzyme E2N	−2.2	6.8×10^{-8}
AW120725	Ubl3	Ubiquitin-like 3	−2.0	4.5×10^{-9}
AI851068	Ubl4	Ubiquitin-like 4	−1.5	4.9×10^{-7}

Notes: *Fold change (FC) is the mean of messenger RNA (mRNA) in old divided by the mean in young ($n = 8$).

†p values were generated by two-way analysis of variance (ANOVA) using multiple testing correction based on the Benjamini and Hochberg False Discovery Rate. Shown are $p < .01$.

A small number of other studies (57–61) have investigated the effects of LT-CR on the heart. Even fewer studies (62–64) have examined the effects of the onset of CR on cardiac physiology and biochemistry.

Our studies differed from other published studies in the use of a young CR group, and groups subjected to short-term shifts in dietary calories. This allowed a more robust analysis of the effects of CR on cardiac gene expression. Our results are novel. Of the age-related changes that we found in gene expression, only 15 have been reported

Table 2. Changed Genes Identified Using Significant Analyses for Microarray (SAM)

Affy ID	GenBank	Gene	Description	Multiclass q Value (%)*	LTCR-FC†	LTCR q Value (%)‡	CR8-FC†	CR8 q Value (%)‡	CON8-FC†	CON8 q Value (%)‡
ECM associated										
101029_f_at	M15501§	Actc1	Actin, α, cardiac 1	0.01	1.3	2.6	1.3	0.6	1.2	54.7
102226_at	AF017639	Cpxm2	Carboxypeptidase X 2 (metallo-carboxypeptidase)	0.01	−1.3	0.9	−1.1	28.9	−1.1	70.2
102227_g_at	AF017639	Cpxm2	Carboxypeptidase X 2	0.01	−1.4	2.5	−1.1	51.5	−1.0	85.3
103817_at	AJ006469	Crtap	Cartilage associated protein	0.01	−1.3	2.6	−1.1	54.8	−1.1	76.8
99669_at	X15986	Lgals1	Lectin, galactose binding, soluble 1	0.59	−1.3	2.6	−1.1	58.0	−1.0	85.3
94305_at	U03419§	Col1a1	Procollagen, type I, α1	0.01	−2.0	0.9	−1.8	2.6	1.3	61.1
101130_at	X58251§	Col1a2	Procollagen, type I, α2	0.01	−9.0	0.9	−1.8	2.6	1.1	88.2
98331_at	X52046§	Col3a1	Procollagen, type III, α1	0.01	−1.3	0.9	−1.4	2.6	1.1	88.2
101110_at	AF064749	Col6a3	Procollagen, type VI, α3	0.01	−1.3	2.6	−1.2	17.1	1.0	92.6
99637_at	AF011450§	Col15a1	Procollagen, type XV	0.01	−1.3	2.6	−1.3	0.8	1.1	85.3
101090_at	L29454	Fbn1	Fibrillin 1	0.01	−1.3	2.6	−1.2	2.6	1.1	91.9
104375_at	AI844853	Spock2	Sparc/osteonectin, cwcv and kazal-like domains proteoglycan 2	0.01	1.6	2.2	1.1	62.6	1.0	64.9
102916_s_at	AB010266	Tnxb	Tenascin XB	0.01	−1.3	2.2	−1.1	58.0	−1.1	78.1
160519_at	U26437	Timp3	Tissue inhibitor of metalloproteinase 3	0.01	1.9	0.9	1.2	73.5	1.1	88.2
Cytoskeleton/cell motility										
94492_at	AB025406	Dstn	Destrin	0.01	1.3	0.9	1.1	70.3	1.2	54.7
93750_at	J04953	Gsn	Gelsolin	0.01	−1.3	2.6	−1.1	62.6	−1.0	88.2
93078_at	X04653	Ly6a	Lymphocyte antigen 6 complex, locus A	0.01	−1.8	0.9	−1.3	27.8	−1.0	88.2
96865_at	M60474	Marcks	Myristoylated alanine rich protein kinase C substrate	0.01	−1.4	0.9	−1.1	29.9	1.0	92.4
93567_at	AW122536	Pfn2	Profilin 2	0.01	−1.6	0.9	−1.1	54.8	−1.1	64.9
94079_at	X61452	Sept4	Septin 4	0.01	−1.3	2.6	−1.2	11.5	−1.0	82.5
98129_at	AI852553§	Tmsb10	Thymosin, beta 10	0.01	−1.5	0.9	−1.4	2.6	1.0	64.9
96426_at	U38967	Ptmb4	Thymosin B4	0.01	−1.3	2.6	−1.3	18.2	1.0	85.3
93541_at	Z68618	Tagln	Transgelin	0.01	1.8	0.9	−1.0	85.5	1.1	82.5
Signal transduction/differentiation/cell division										
102321_at	M93422	Adcy6	Adenylate cyclase 6	0.01	1.4	0.9	1.1	10.7	1.1	8.0
98924_at	Y08027	Art3	ADP-ribosyltransferase 3	0.01	2.0	0.9	1.1	85.5	−1.0	89.7
96146_at	D83745	Btg3	B-cell translocation gene 3	0.01	3.2	0.9	−1.1	50.4	−1.0	85.3
100555_at	AI846152§	Dscr1	Calcipressin 1	0.01	−1.5	0.9	−2.1	2.6	−1.2	64.9
102736_at	M19681§	Ccl2	Chemokine (C-C motif) ligand 2	0.01	−1.7	0.9	−1.4	0.8	−1.1	82.5
94761_at	X70058§	Ccl7	Chemokine (C-C motif) ligand 7	0.01	−1.5	0.9	−1.5	2.6	−1.2	64.9
92777_at	M32490§	Cyr61	Cysteine-rich, angiogenic inducer, 61	0.01	−2.6	0.9	−1.7	2.6	−1.2	14.1
162234_f_at	AV139913	Cxcl12	Chemokine (C-X-C motif) ligand 12	0.01	−1.7	0.9	−1.1	36.3	1.0	62.5
94881_at	AW048937	Cdkn1a	Cyclin-dependent kinase inhibitor 1A (P21)	0.01	1.7	0.9	−1.1	54.8	−1.1	78.6
102217_at	AI639925§	Gprk5	G protein-coupled receptor kinase 5	0.01	−2.3	0.9	−1.3	0.8	−1.1	76.8
98465_f_at	M31419	Ifi16	Interferon γ-inducible protein 16	0.01	−1.4	0.9	−1.2	27.8	−1.0	89.7
94224_s_at	M74123	Ifi205	Interferon activated gene 205	0.01	−2.3	0.9	−1.2	8.0	−1.1	82.5
160253_at	AW125390§	Ifitm3	Interferon induced transmembrane protein 3	0.01	−1.8	0.9	−1.3	1.5	−1.0	89.7
100307_at	AA002843	Lyl1	Lymphoblastomic leukemia	0.01	5.9	0.9	1.1	85.6	1.2	79.3
101487_f_at	U47737§	Ly6e	Lymphocyte antigen 6 complex, locus E	0.01	−2.3	0.9	−2.6	2.6	−1.0	89.7
93253_at	D87271	Mapk1	Mitogen activated protein kinase 1	0.07	−1.3	0.9	−1.2	40.7	−1.1	64.9
104184_at	D16497§,‖	Nppb	Natriuretic peptide precursor type B	0.01	−2.7	0.9	−2.1	2.6	−1.9	0.6
160819_at	AW121600	Ndrg4	N-myc downstream regulated gene 4	0.01	1.4	4.1	1.1	85.5	1.2	78.6
98507_at	AI834950	Nr1d1 (reverbAα)	Nuclear receptor subfamily 1, group D, member 1	0.01	−1.3	3.5	−1.1	51.5	−1.2	64.9
102668_at	X57638	Ppara	Peroxisome proliferator activated receptor α	0.01	1.3	0.9	1.1	40.7	1.0	85.3
98005_at	AW125442	Pkia	Protein kinase inhibitor α	0.01	−1.3	0.9	−1.1	51.5	−1.0	82.5
94003_at	AI848510	Prkwnk1	Protein kinase, lysine deficient 1	0.01	−1.3	2.5	−1.1	60.8	1.0	89.7
98007_at	AJ131021	Rps6ka2	Ribosomal protein S6 kinase, polypeptide 2	0.01	−2.2	0.9	−1.1	40.8	−1.0	78.6
104374_at	M64086	Serpina3n	Serine (or cysteine) proteinase inhibitor, clade A, member 3N	0.01	−1.3	4.1	−1.2	10.7	−1.2	64.9
95731_at	AI843106	Sesn1	Sestrin 1	0.01	1.9	0.9	1.0	85.5	1.0	80.4

Table 2. Changed Genes Identified Using Significant Analyses for Microarray (SAM) (*Continued*)

Affy ID	GenBank	Gene	Description	Multiclass q Value (%)*	LTCR-FC†	LTCR q Value (%)‡	CR8-FC†	CR8 q Value (%)‡	CON8-FC†	CON8 q Value (%)‡
Immune/inflammation										
96020_at	M22531	C1qb	Complement component 1, q subcomponent, β polypeptide	0.07	−1.4	3.3	−1.2	24.0	−1.0	85.8
92223_at	X66295	C1qg	Complement component 1, q subcomponent, γ polypeptide	0.01	−2.2	0.9	−1.1	28.9	−1.1	76.8
92866_at	X52643	H2-Aa	Histocompatibility 2, class II antigen A, α	0.07	−1.5	2.2	−1.2	14.9	1.0	14.1
97173_f_at	M27134	H2-K2	Histocompatibility 2, K region locus 2	0.01	−1.6	0.9	−1.1	40.8	1.1	69.9
101054_at	X00496§	Ii	Ia-associated invariant chain	0.01	−4.7	0.9	−1.9	2.6	1.1	92.6
93894_f_at	U49866	Klra9	Killer cell lectin-like receptor, subfamily A, member 9	0.01	−1.3	0.9	−1.1	40.7	−1.2	14.1
99081_at	AF010254	Serping1	Serine (or cysteine) proteinase inhibitor, clade G, member 1	2.02	−1.3	4.1	−1.2	18.2	−1.1	78.1
Stress/chaperone										
101955_at	AJ002387	Hspa5	Heat shock 70kd protein 5 (GRP78)	0.01	−1.3	0.9	−1.1	10.7	−1.0	8.0
95057_at	AI846938	Herpud1	Homocysteine-inducible, ER stress-inducible, ubiquitin-like domain member 1	0.01	2.0	0.9	1.2	75.3	1.1	80.4
94209_g_at	AW045202	Txndc7	Thioredoxin domain containing 7	0.01	−1.3	2.6	−1.2	40.8	1.0	82.5
Carbohydrate/energy metabolism										
97489_at	AI846739	Pygb	Brain glycogen phosphorylase	0.01	−1.3	3.3	−1.0	82.8	−1.0	85.3
101058_at	J00356‖	Amy1	Mouse α-amylase-1	0.07	−1.3	2.6	−1.1	55.2	−1.3	0.6
Lipid metabolism										
103401_at	L11163	Acads	Acyl-Coenzyme A dehydrogenase, short chain	0.07	−1.3	3.8	−1.1	43.6	−1.0	88.2
97235_f_at	AW124988	Apobec2	Apolipoprotein B editing complex 2	0.01	2.4	0.9	1.2	60.8	1.2	62.0
101538_i_at	AW226939	Ces3	Carboxylesterase 3	0.01	−2.8	0.9	−1.1	55.2	−1.0	89.7
95646_at	U01170	Cpt2	Carnitine palmitoyltransferase 2	0.01	−1.3	3.3	−1.1	43.6	1.0	80.4
101867_at	U11680	Gpam	Glycerol-3-phosphate acyltransferase	0.01	−1.3	2.5	−1.2	14.9	−1.1	76.8
160083_at	M63335	Lpl	Lipoprotein lipase	0.01	1.4	2.2	1.1	82.8	1.2	54.7
103581_at	Y14004	Cte1	Peroxisomal acyl-CoA thioesterase 1	0.01	2.8	0.9	1.1	86.1	1.2	62.0
100927_at	U28960	Pltp	Phospholipid transfer protein	0.07	−1.3	3.3	−1.1	55.2	1.1	88.2
94056_at	M21285	Scd1	Stearoyl-Coenzyme A desaturase 1	0.07	4.5	0.9	3.7	47.2	4.0	54.7
Xenobiotic/oxidant/toxicant metabolism										
104011_at	AB017482	Aox1	Aldehyde oxidase 1	0.01	−1.3	2.6	−1.1	50.4	−1.1	67.6
98079_at	AB005450	Car14	Carbonic anhydrase 14	0.01	1.5	0.9	1.2	14.9	1.1	64.9
96346_at	AI854020	Cdo1	Cysteine dioxygenase 1, cytosolic	0.01	1.8	0.9	1.1	50.4	1.1	85.3
93996_at	X01026§	Cyp2e1	Cytochrome P450, family 2, subfamily e, polypeptide 1	0.01	2.8	0.9	1.3	2.6	1.3	43.1
95944_at	AV299153	Dhx36	DEAD box polypeptide 36	0.07	1.4	3.5	1.1	85.5	1.1	82.5
99872_s_at	L39879	Ftl1	Ferritin light chain 1	0.16	−1.3	2.2	−1.2	40.7	−1.0	85.3
104500_at	L34111	Idua	Iduronidase, alpha-L-	0.01	2.8	0.9	1.1	82.8	1.0	64.9
97055_s_at	AI118194	Prdx1	Peroxiredoxin 1	0.01	−1.3	2.6	−1.1	54.8	−1.0	88.2
97758_at	AB023564	Prdx1	Peroxiredoxin 1	0.01	−1.3	2.2	−1.1	54.8	−1.0	88.2
103087_at	L02331	Sult1a1	Sulfotransferase family 1A, phenol-preferring, member 1	0.01	2.0	0.9	1.0	86.1	−1.1	67.6
99111_at	U09874	Skd3	Suppressor of K+ transport defect 3	0.01	−1.7	0.9	−1.1	40.8	−1.1	67.6
97402_at	M88694§	Temt	Thioether S-methyltransferase	0.01	1.7	0.9	1.8	2.6	−1.1	74.5
EST/unknown										
95749_at	AW122364	Armet	Arginine-rich, mutated in early stage tumors	0.01	−1.3	3.3	−1.2	22.7	−1.1	76.8
94820_r_at	AF005886§	Ccni	Cyclin I	0.01	1.4	3.3	1.3	2.6	1.2	54.7
96912_s_at	X15591	Ctla2a	Cytotoxic T lymphocyte-associated protein 2α	0.01	−2.4	0.9	−1.1	85.5	−1.0	92.4
97426_at	X98471	Emp1	Epithelial membrane protein 1	0.01	−1.7	0.9	−1.2	11.5	1.0	92.6
93028_at	X58196	H19	H19 fetal liver mRNA	0.01	3.0	0.9	1.0	14.9	1.3	29.4
97485_at	AI850953	Pcyox1	Prenylcysteine lyase	0.01	−1.3	2.6	−1.1	70.3	1.0	92.6
160896_at	D13003	Rcn	Reticulocalbin	0.01	−1.3	0.9	−1.2	10.7	−1.1	64.9
98624_at	X75316	Rnpc1	RNA-binding region (RNP1, RRM) containing 1	0.01	1.3	0.9	1.1	65.1	1.0	92.2

Table 2. Changed Genes Identified Using Significant Analyses for Microarray (SAM) (*Continued*)

Affy ID	GenBank	Gene	Description	Multiclass q Value (%)*	LTCR-FC†	LTCR q Value (%)‡	CR8-FC†	CR8 q Value (%)‡	CON8-FC†	CON8 q Value (%)‡
98033_at	AA710132	EST		0.01	−1.3	3.2	−1.1	66.9	−1.1	64.9
97349_at	AA727410	EST		0.07	−1.3	2.6	−1.1	40.7	−1.1	64.9
96135_at	AA833425	EST		0.01	1.9	0.9	1.2	34.3	1.1	85.3
96785_at	AF110520	EST		0.01	−1.3	4.1	−1.2	11.5	1.0	91.9
100877_at	AI194274	EST		0.01	−1.3	2.2	−1.2	18.2	−1.1	64.9
92202_g_at	AI553024§	EST		0.01	2.5	0.9	1.6	1.9	1.4	54.7
93155_at	AI847069	EST		0.01	1.3	2.6	1.1	47.2	1.2	54.7
103743_at	AI851348	EST		0.01	−1.3	2.6	−1.1	43.6	−1.1	54.7
160835_i_at	AI851695	EST		0.01	2.4	0.9	1.1	65.1	1.1	54.7
96686_i_at	AI853864	EST		0.01	−1.3	2.6	−1.1	65.1	−1.1	70.2
161184_f_at	AV235418	EST		0.01	−1.3	2.6	−1.1	55.2	1.1	62.5
161817_f_at	AV376312	EST		0.01	1.9	0.9	1.0	55.2	1.0	62.5
100058_at	AW047776§	EST		0.01	−1.3	2.6	−1.3	0.8	−1.1	54.7
96791_at	AW047875	EST		0.01	−1.3	0.9	−1.2	11.5	1.1	64.9
96953_at	AW120786‖	EST		0.01	−1.4	0.9	−1.2	10.7	−1.3	0.6
98594_at	AW125453	EST		0.01	−1.3	2.6	−1.1	27.8	−1.1	64.9
99849_at	C85523	EST		0.01	1.4	2.6	1.2	45.1	1.1	91.6

Notes: *Multiclass q value is the lowest False Discovery Rate at which a change in gene expression is statistically significant. It is similar to a *p* value, but is adapted for the simultaneous analysis of large gene sets using SAM. Values were generated by multiclass SAM of the old-long-term control (LTCON), old-long-term calorie-restricted (LTCR), 8 weeks of CR (CR8), and LTCR mice shifted to control feeding for 8 weeks (CON8) groups.

†Fold change (FC) is mean expression level of a messenger RNA (mRNA) in old-LTCR, old-CR8, or old-CON8 mice divided by that in old-LTCON mice ($n = 4$).

‡q values for the FC from old-LTCR, old-CR8, or old-CON8. Values were generated by two-class unpaired SAM.

§Genes for which the LTCR-induced changes in gene expression were reproduced in CR8 mice.

‖LTCR-responsive transcripts which did not return to control levels of expression in CON8 mice.

ECM = extracellular matrix; ADP = adenosine diphosphate; DEAD = asparagine, glutamine, alanine, asparagine domain; RNP1 = ribonucleoprotein 1; RRM = RNA recognition motif; EST = expressed sequence tag.

previously (Supplementary Table 8) (56). Of the 152 LTCR-related changes that we found in gene expression (Figure 2), just 33 (of 831 changes reported by others) had been found previously (Supplementary Table 9) (56). We did not find CR-related changes consistent with reduced endogenous DNA damage (56).

The dissimilarities between our results and those of others may be due to the use of different analytical techniques. Nonidentical overlapping sets of genes are commonly identified using alternative methods of data analysis, even using identical data sets (27). The Robust Multichip Average analysis, SAM, and ANOVA used here are conservative, widely utilized, and accepted. It is possible that the genes reported by others were altered, but were not statistically significant in our analysis. We verified nine gene changes of nine randomly chosen changed genes using qPCR. Thus, the changed genes reported here likely represent true positives.

Conclusion

Long-term CR affected few of the many genes changed by aging, suggesting that most of these genes are not involved in the cardioprotective effects of CR. In contrast, CR8, which decreases age-associated mortality and increases life span, reproduced 19% of the LTCR-responsive changes in gene expression found using SAM. Eight weeks of control feeding returned 97% of the LTCR-responsive genes to control levels. Thus, genes which change expression with LTCR respond rapidly to caloric intake, consistent with the idea that CR produces important effects on the heart by rapidly shifting gene expression toward a state of reduced cardiac remodeling and fibrosis and enhanced contractility and energy generation via lipid β-oxidation.

Acknowledgments

This work was supported by unrestricted gifts from the Life Extension Foundation.

Dr. Dhahbi is now with BioMarker Pharmaceuticals, Inc., Alameda, CA.

Dr. Tsuchiya is now with the Department of Pathology & Gerontology, Nagasaki University Graduate School of Biomedical Science, Japan.

Dr. Kim is now with the School of Medicine, University of California, Los Angeles.

Address correspondence to Stephen R. Spindler, PhD, Department of Biochemistry, University of California–Riverside, 3401 Watkins Dr., Riverside, CA 92521. E-mail: spindler@ucr.edu

References

1. Weisfeldt M. Aging, changes in the cardiovascular system, and responses to stress. *Am J Hypertens*. 1998;11:41S–45S.
2. McGuire DK, Levine BD, Williamson JW, et al. A 30-year follow-up of the Dallas Bedrest and Training Study: I. Effect of age on the cardiovascular response to exercise. *Circulation*. 2001;104:1350–1357.
3. Turturro A, Duffy P, Hass B, Kodell R, Hart R. Survival characteristics and age-adjusted disease incidences in C57BL/6 mice fed a commonly used cereal-based diet modulated by dietary restriction. *J Gerontol Biol Sci*. 2002;57A:B379–B389.
4. Edwards MG, Sarkar D, Klopp R, Morrow JD, Weindruch R, Prolla TA. Age-related impairment of the transcriptional responses to oxidative stress in the mouse heart. *Physiol Genomics*. 2003;13:119–127.
5. Anversa P, Palackal T, Sonnenblick EH, Olivetti G, Meggs LG, Capasso JM. Myocyte cell loss and myocyte cellular hyperplasia in the hypertrophied aging rat heart. *Circ Res*. 1990;67:871–885.
6. Eghbali M, Eghbali M, Robinson TF, Seifter S, Blumenfeld OO. Collagen accumulation in heart ventricles as a function of growth and aging. *Cardiovasc Res*. 1989;23:723–729.

7. De Souza RR. Aging of myocardial collagen. *Biogerontology*. 2002; 3:325–335.
8. Janicki JS. Myocardial collagen remodeling and left ventricular diastolic function. *Braz J Med Biol Res*. 1992;25:975–982.
9. Varagic J, Susic D, Frohlich E. Heart, aging, and hypertension. *Curr Opin Cardiol*. 2001;16:336–341.
10. Colucci WS. Molecular and cellular mechanisms of myocardial failure. *Am J Cardiol*. 1997;80:15L–25L.
11. Lushnikova EL, Nepomnyashchikh LM, Klinnikova MG. Morphological characteristics of myocardial remodeling during compensatory hypertrophy in aging Wistar rats. *Bull Exp Biol Med*. 2001;132:1201–1206.
12. Lakatta EG. Cardiovascular aging in health. *Clin Geriatr Med*. 2000; 16:419–444.
13. Moreau R, Heath SH, Doneanu CE, Harris RA, Hagen TM. Age-related compensatory activation of pyruvate dehydrogenase complex in rat heart. *Biochem Biophys Res Commun*. 2004;325:48–58.
14. van Raalte DH, Li M, Pritchard PH, Wasan KM. Peroxisome proliferator-activated receptor (PPAR)-alpha: a pharmacological target with a promising future. *Pharm Res*. 2004;21:1531–1538.
15. Dhahbi JM, Kim HJ, Mote PL, Beaver RJ, Spindler SR. Temporal linkage between the phenotypic and genomic responses to caloric restriction. *Proc Natl Acad Sci U S A*. 2004;101:5524–5529.
16. Mair W, Goymer P, Pletcher SD, Partridge L. Demography of dietary restriction and death in Drosophila. *Science*. 2003;301:1731–1733.
17. Smith JV, Heilbronn LK, Ravussin E. Energy restriction and aging. *Curr Opin Clin Nutr Metab Care*. 2004;7:615–622.
18. Wagh A, Stone NJ. Treatment of metabolic syndrome. *Expert Rev Cardiovasc Ther*. 2004;2:213–228.
19. Cao SX, Dhahbi JM, Mote PL, Spindler SR. Genomic profiling of short- and long-term caloric restriction effects in the liver of aging mice. *Proc Natl Acad Sci U S A*. 2001;98:10630–10635.
20. Dhahbi JM, Mote PL, Cao SX, Spindler SR. Hepatic gene expression profiling of streptozotocin-induced diabetes. *Diabetes Technol Ther*. 2003;5:411–420.
21. Irizarry RA, Bolstad BM, Collin F, Cope LM, Hobbs B, Speed TP. Summaries of Affymetrix GeneChip probe level data. *Nucleic Acids Res*. 2003;31:e15.
22. Affymetrix I. New Statistical Algorithms for Monitoring Gene Expression on GeneChip Probe Arrays. *Technical Notes 1, Part No 701097 Rev 1*. 2001.
23. Tusher VG, Tibshirani R, Chu G. Significance analysis of microarrays applied to the ionizing radiation response. *Proc Natl Acad Sci U S A*. 2001;98:5116–5121.
24. Seeland U, Haeuseler C, Hinrichs R, et al. Myocardial fibrosis in transforming growth factor-beta(1) (TGF-beta(1)) transgenic mice is associated with inhibition of interstitial collagenase. *Eur J Clin Invest*. 2002;32:295–303.
25. Junqueira LC, Bignolas G, Brentani RR. Picrosirius staining plus polarization microscopy, a specific method for collagen detection in tissue sections. *Histochem J*. 1979;11:447–455.
26. Junqueira LC, Cossermelli W, Brentani R. Differential staining of collagens type I, II and III by Sirius Red and polarization microscopy. *Arch Histol Jpn*. 1978;41:267–274.
27. Rosati B, Grau F, Kuehler A, Rodriguez S, McKinnon D. Comparison of different probe-level analysis techniques for oligonucleotide microarrays. *Biotechniques*. 2004;36:316–322.
28. Heilbronn LK, Ravussin E. Calorie restriction and aging: review of the literature and implications for studies in humans. *Am J Clin Nutr*. 2003;78:361–369.
29. Fontana L, Meyer TE, Klein S, Holloszy JO. Long-term calorie restriction is highly effective in reducing the risk for atherosclerosis in humans. *Proc Natl Acad Sci U S A*. 2004;101:6659–6663.
30. Nakagawa O, Ogawa Y, Itoh H, et al. Rapid transcriptional activation and early mRNA turnover of brain natriuretic peptide in cardiocyte hypertrophy. Evidence for brain natriuretic peptide as an ''emergency'' cardiac hormone against ventricular overload. *J Clin Invest*. 1995;96: 1280–1287.
31. Luchner A, Muders F, Dietl O, et al. Differential expression of cardiac ANP and BNP in a rabbit model of progressive left ventricular dysfunction. *Cardiovasc Res*. 2001;51:601–607.
32. Tsutamoto T, Wada A, Maeda K, et al. Attenuation of compensation of endogenous cardiac natriuretic peptide system in chronic heart failure: prognostic role of plasma brain natriuretic peptide concentration in patients with chronic symptomatic left ventricular dysfunction. *Circulation*. 1997;96:509–516.
33. Raizada V, Thakore K, Luo W, McGuire PG. Cardiac chamber-specific alterations of ANP and BNP expression with advancing age and with systemic hypertension. *Mol Cell Biochem*. 2001;216:137–140.
34. Yang CL, Angell J, Mitchell R, Ellison DH. WNK kinases regulate thiazide-sensitive Na-Cl cotransport. *J Clin Invest*. 2003;111:1039–1045.
35. Lane MA, Tilmont EM, De Angelis H, et al. Short-term calorie restriction improves disease-related markers in older male rhesus monkeys (Macaca mulatta). *Mech Ageing Dev*. 2000;112:185–196.
36. Capstick F, Brooks BA, Burns CM, Zilkens RR, Steinbeck KS, Yue DK. Very low calorie diet (VLCD): a useful alternative in the treatment of the obese NIDDM patient. *Diabetes Res Clin Pract*. 1997;36:105–111.
37. Nadal-Ginard B, Kajstura J, Leri A, Anversa P. Myocyte death, growth, and regeneration in cardiac hypertrophy and failure. *Circ Res*. 2003;92: 139–150.
38. Takeishi Y, Huang Q, Abe J, et al. Activation of mitogen-activated protein kinases and p90 ribosomal S6 kinase in failing human hearts with dilated cardiomyopathy. *Cardiovasc Res*. 2002;53:131–137.
39. Pillarisetti K, Gupta SK. Cloning and relative expression analysis of rat stromal cell derived factor-1 (SDF-1)1: SDF-1 alpha mRNA is selectively induced in rat model of myocardial infarction. *Inflammation*. 2001;25:293–300.
40. Lloyd S, Brocks C, Chatham JC. Differential modulation of glucose, lactate, and pyruvate oxidation by insulin and dichloroacetate in the rat heart. *Am J Physiol Heart Circ Physiol*. 2003;285:H163–H172.
41. McMillin JB, Taffet GE, Taegtmeyer H, Hudson EK, Tate CA. Mitochondrial metabolism and substrate competition in the aging Fischer rat heart. *Cardiovasc Res*. 1993;27:2222–2228.
42. Iemitsu M, Miyauchi T, Maeda S, et al. Aging-induced decrease in the PPAR-alpha level in hearts is improved by exercise training. *Am J Physiol Heart Circ Physiol*. 2002;283:H1750–H1760.
43. Karbowska J, Kochan Z, Smolenski RT. Peroxisome proliferator-activated receptor alpha is downregulated in the failing human heart. *Cell Mol Biol Lett*. 2003;8:49–53.
44. Kassam A, Capone JP, Rachubinski RA. Orphan nuclear hormone receptor RevErbalpha modulates expression from the promoter of the hydratase-dehydrogenase gene by inhibiting peroxisome proliferator-activated receptor alpha-dependent transactivation. *J Biol Chem*. 1999; 274:22895–22900.
45. Hunt MC, Lindquist PJG, Peters JM, Gonzalez FJ, Diczfalusy U, Alexson SE. Involvement of the peroxisome proliferator-activated receptor α in regulating long-chain acyl-CoA thioesterases. *J Lipid Res*. 2000;41:814–823.
46. Schoonjans K, Peinado-Onsurbe J, Lefebvre AM, et al. PPARalpha and PPARgamma activators direct a distinct tissue-specific transcriptional response via a PPRE in the lipoprotein lipase gene. *EMBO J*. 1996;15: 5336–5348.
47. Tepe NM, Lorenz JN, Yatani A, et al. Altering the receptor-effector ratio by transgenic overexpression of type V adenylyl cyclase: enhanced basal catalytic activity and function without increased cardiomyocyte beta-adrenergic signalling. *Biochemistry*. 1999;38: 16706–16713.
48. Gao MH, Bayat H, Roth DM, et al. Controlled expression of cardiac-directed adenylylcyclase type VI provides increased contractile function. *Cardiovasc Res*. 2002;56:197–204.
49. Vinge LE, Oie E, Andersson Y, Grogaard HK, Andersen G, Attramadal H. Myocardial distribution and regulation of GRK and beta-arrestin isoforms in congestive heart failure in rats. *Am J Physiol Heart Circ Physiol*. 2001;281:H2490–H2499.
50. Tailleux A, Torpier G, Mezdour H, Fruchart JC, Staels B, Fievet C. Murine models to investigate pharmacological compounds acting as ligands of PPARs in dyslipidemia and atherosclerosis. *Trends Pharmacol Sci*. 2003;24:530–534.
51. Pineda Torra I, Gervois P, Staels B. Peroxisome proliferator-activated receptor alpha in metabolic disease, inflammation, atherosclerosis and aging. *Curr Opin Lipidol*. 1999;10:151–159.
52. Towbin JA, Bowles NE. Genetic abnormalities responsible for dilated cardiomyopathy. *Curr Cardiol Rep*. 2000;2:475–480.
53. Rao VU, Spinale FG. Controlling myocardial matrix remodeling: implications for heart failure. *Cardiol Rev*. 1999;7:136–143.

54. Nadal-Ginard B, Kajstura J, Leri A, Anversa P. Myocyte death, growth, and regeneration in cardiac hypertrophy and failure. *Circ Res.* 2003; 92:139–150.
55. Chang KT, Min KT. Regulation of lifespan by histone deacetylase. *Ageing Res Rev.* 2002;1:313–326.
56. Lee CK, Allison DB, Brand J, Weindruch R, Prolla TA. Transcriptional profiles associated with aging and middle age-onset caloric restriction in mouse hearts. *Proc Natl Acad Sci U S A.* 2002;99:14988–14993.
57. Shiojima I, Yefremashvili M, Luo Z, et al. Akt signaling mediates postnatal heart growth in response to insulin and nutritional status. *J Biol Chem.* 2002;277:37670–37677.
58. Taffet GE, Pham TT, Hartley CJ. The age-associated alterations in late diastolic function in mice are improved by caloric restriction. *J Gerontol A Biol Sci.* 1997;52A:B285–B290.
59. Leeuwenburgh C, Wagner P, Holloszy JO, Sohal RS, Heinecke JW. Caloric restriction attenuates dityrosine cross-linking of cardiac and skeletal muscle proteins in aging mice. *Arch Biochem Biophys.* 1997; 346:74–80.
60. Swoap SJ, Haddad F, Bodell P, Baldwin KM. Control of beta-myosin heavy chain expression in systemic hypertension and caloric restriction in the rat heart. *Am J Physiol.* 1995;269:C1025–C1033.
61. Drew B, Phaneuf S, Dirks A, et al. Effects of aging and caloric restriction on mitochondrial energy production in gastrocnemius muscle and heart. *Am J Physiol Regul Integr Comp Physiol.* 2003;284:R474–R480.
62. Pamplona R, Portero-Otin M, Requena J, Gredilla R, Barja G. Oxidative, glycoxidative and lipoxidative damage to rat heart mitochondrial proteins is lower after 4 months of caloric restriction than in age-matched controls. *Mech Ageing Dev.* 2002;123:1437–1446.
63. Gredilla R, Lopez-Torres M, Barja G. Effect of time of restriction on the decrease in mitochondrial H2O2 production and oxidative DNA damage in the heart of food-restricted rats. *Microsc Res Tech.* 2002;59: 273–277.
64. Selman C, Gredilla R, Phaneuf S, Kendaiah S, Barja G, Leeuwenburgh C. Short-term caloric restriction and regulatory proteins of apoptosis in heart, skeletal muscle and kidney of Fischer 344 rats. *Biogerontology.* 2003;4:141–147.

Received January 11, 2005
Accepted August 22, 2005
Decision Editor: James R. Smith, PhD